POLITECNICO DI TORINO
Repository ISTITUZIONALE

Dipolar-induced resonance for ultracold bosons in a quasi-one-dimensional optical lattice

Original
Dipolar-induced resonance for ultracold bosons in a quasi-one-dimensional optical lattice / Bartolo, N.; Papoular, D. J.; Barbiero, L.; Menotti, C.; Recati, A.. - In: PHYSICAL REVIEW A. - ISSN 1050-2947. - ELETTRONICO. - 88:2(2013). [10.1103/PhysRevA.88.023603]

Availability:
This version is available at: 11583/2948166 since: 2022-01-02T10:38:29Z

Publisher:
AMER PHYSICAL SOC

Published
DOI:10.1103/PhysRevA.88.023603

Terms of use:

This article is made available under terms and conditions as specified in the corresponding bibliographic description in the repository

Publisher copyright

(Article begins on next page)

12 October 2024

Dipolar-induced resonance for ultracold bosons in a quasi-one-dimensional optical lattice

N. Bartolo,[1,2] D. J. Papoular,[1] L. Barbiero,[3,4] C. Menotti,[1] and A. Recati[1]
[1]*INO-CNR BEC Center and Dipartimento di Fisica, Università di Trento, 38123 Povo, Italy*
[2]*Laboratoire Charles Coulomb, CNRS, Université Montpellier 2, Montpellier, France*
[3]*Dipartimento di Fisica e Astronomia "Galileo Galilei", Universita di Padova, Padova, Italy*
[4]*Laboratoire de Physique Théorique, CNRS, Université de Toulouse, Toulouse, France*
(Received 18 March 2013; published 6 August 2013)

We study the role of the dipolar-induced resonance (DIR) in a quasi-one-dimensional system of ultracold bosons. We first describe the effect of the DIR on two particles in a harmonic trap. Then, we consider a deep optical lattice loaded with ultracold dipolar bosons. In order to describe this system, we introduce a novel atom-dimer extended Bose-Hubbard model, which is the minimal model correctly accounting for the DIR. We analyze the impact of the DIR on the phase diagram at $T = 0$ by exact diagonalization of a small-sized system. We show that the DIR strongly affects this phase diagram. In particular, we predict the mass density wave to occur in a narrow domain corresponding to weak nearest-neighbor interactions, and we predict the occurrence of a collapse phase for stronger dipolar interactions.

DOI: 10.1103/PhysRevA.88.023603 PACS number(s): 03.75.Hh, 05.30.Jp, 34.50.−s, 37.10.Jk

I. INTRODUCTION

The recent experimental developments in the field of ultracold dipolar gases have opened up fascinating prospects for the study of systems exhibiting dipole–dipole interaction (DDI) [1,2]. Bose-Einstein Condensates (BECs) of magnetic atoms have been realized using chromium [3], erbium [4], and dysprosium [5]. However, atomic magnetic moments are small ($\lesssim 10\,\mu_B$, where μ_B is the Bohr magneton), and therefore the effects of the DDI observed with these systems have remained perturbative up to now [6]. The recent realization of the ultracold heteronuclear molecules RbK [7] and NaK [8], which both carry electric dipole moments of the order of 1 D, offers a promising route towards stronger DDI effects, but quantum degeneracy still remains to be achieved with these systems. Rydberg atoms boast much larger dipole moments but yield challenging experimental problems associated with time and length scales [9].

The DDI is anisotropic and long ranged, and dipolar gases thus allow for the quantum simulation of more general Hamiltonians than those accessible with nondipolar neutral particles, whose interaction is described by the standard s-wave interaction [10]. Trapping a dipolar system into lower dimensions stabilizes it with respect to two-body [11] and many-body [12] instabilities caused by the attractive part of the three-dimensional (3D) DDI. This has prompted detailed studies of dipolar systems in 2D and quasi-2D [13,14], bilayer [15], and quasi-1D [16–19] geometries.

Experiments involving dipolar bosons in optical lattices have recently been performed both with atomic BECs [20] and noncondensed dipolar molecules [21,22]. Up to now, their standard theoretical description has relied on the extended Bose-Hubbard model (EBHM) accounting for the interaction between nearest and more distant neighbors [1]. The 1D EBHM has revealed the occurrence, beyond the standard Mott-insulator (MI) and superfluid (SF) phases, of a mass density wave (MDW) phase [18,23] and a Haldane insulator phase [24,25].

The proper description of specific atomic systems by lattice models such as the EBHM requires a careful mapping between models and physical systems. This has already been pointed out for the Hubbard model [26], but the nontrivial effects associated with long-range and anisotropic interactions are even more important. As a first step in this direction, we analyze the important role played by the dipolar–induced resonance (DIR) [27,28], which is a low-energy resonance occurring when the dipole strength is varied. We show that the DIR affects both the two-body and the many-body physics of the system (see, e.g. Ref. [29] about the BEC-BCS crossover).

In this article, we consider a quasi-1D lattice system of bosonic dipoles in the tight-binding regime [30,31].[1] We assume that the dipole moments are aligned perpendicularly to the trap axis. In this situation, a single DIR occurs. Accounting for it requires going beyond the single-band EBHM. We develop an atom-dimer EBHM, which is the minimal model capturing the DIR. Even at this level, we find that the DIR has a strong impact on the many-body phase diagram as compared to previous descriptions [23,25].

The scattering and bound-state properties of the DDI have been studied numerically for free-space models [32] and for 3D and 2D lattice systems [33]. In our quasi-1D geometry, we model the DDI using an effective potential obtained by averaging the transverse degrees of freedom into the harmonic-oscillator ground state [16,17]:

$$V_{1D}(x) = \left(g_{1D} - \frac{\hbar^2}{m}\frac{2\,r^*}{3\,l_\perp^2}\right)\delta(x) + \frac{\hbar^2}{m}\frac{r^*}{l_\perp^3}\left[\sqrt{\frac{\pi}{8}}\,e^{\frac{1}{2}\frac{x^2}{l_\perp^2}}\left(\frac{x^2}{l_\perp^2}+1\right) \times \mathrm{Erfc}\left(\frac{|x|}{\sqrt{2}l_\perp}\right) - \frac{|x|}{2\,l_\perp}\right], \quad (1)$$

where $r^* = mD^2/\hbar^2$ is the dipolar length, with D being the dipolar strength. The range of this potential is determined by the oscillator length $l_\perp = (\hbar/m\omega_\perp)^{1/2}$ in the strongly

[1]Our analysis holds for both atomic and molecular dipoles.

 ©2013 American Physical Society

confined directions y and z. The term $g_{1D} = 2\hbar^2 a_{3D}/ml_\perp^2$ is the strength of the s-wave contact interaction for a 3D scattering length a_{3D} [34], which can be manipulated using a Feshbach resonance [35]. It competes with the DDI to determine the stability and the phase of the system [36]. We assume $g_{1D} = 0$ unless otherwise specified. Under this assumption, Eq. (1) still contains a contact term proportional to r^*. The use of Eq. (1) amounts to neglecting the role of confinement-induced resonances [37]. Their interplay with the DIR might lead to even richer physics, which we are currently investigating.

II. TWO-BODY PHYSICS

The basic building block of our many-body lattice Hamiltonian [Eq. (4)] is provided by the solution of the two-body problem in a single lattice site. Hence, we solve for the ground-state of two dipolar bosons in a 1D harmonic well, with the trapping frequency ω_0 and the oscillator length $l_0 = (\hbar/m\omega_0)^{1/2}$. The center-of-mass and relative motions are decoupled, and the relative motion is governed by the following Hamiltonian:

$$H_{2B} = \frac{p^2}{2m_r} + \frac{1}{2}m_r\omega_0^2 x^2 + V_{1D}(x), \tag{2}$$

where x is the interparticle distance, p is its conjugate momentum, and $m_r = m/2$ is the reduced mass.

Unlike for the contact interaction [38], the Hamiltonian H_{2B} cannot be diagonalized analytically. We seek its ground state numerically, by considering the restriction of H_{2B} onto a subspace spanned by a finite number of basis states $\{|\phi_n\rangle\}$. Depending on the value of r^*, V_{1D} supports either no bound state or a single one. The bound state is present for large enough values of r^*, and its entrance coincides with the occurrence of the DIR. The "bare" bound state supported by the attractive contact part of $V_{1D}(x)$ plays a key role. Its wave function is $\psi_{BS}(x) = \sqrt{\kappa}\exp(-\kappa|x|)$, where $\kappa = r^*/(3l_\perp^2)$, and its cusp at $x = 0$ cannot be reproduced by projecting $|\psi_{BS}\rangle$ onto any finite number of harmonic oscillator eigenstates which are all smooth at $x = 0$. Hence, the DIR physics can only be captured if a wave function which has a cusp at $x = 0$ is included in the basis $\{|\phi_n\rangle\}$. The smallest such basis is $\{|\phi_0\rangle, |\phi_{-1}\rangle\}$, where $|\phi_0\rangle$ is the ground state of the 1D harmonic oscillator with frequency ω_0, and $|\phi_{-1}\rangle \propto |\psi_{BS}\rangle - \langle\phi_0|\psi_{BS}\rangle|\phi_0\rangle$ is a linear combination of $|\psi_{BS}\rangle$ and $|\phi_0\rangle$ chosen such that the basis is orthonormal. Hence, for a given value of r^*, we replace H_{2B} by the following two-state Hamiltonian:

$$H_{2\text{state}} = \begin{pmatrix} \langle\phi_0|H_{2B}|\phi_0\rangle & \langle\phi_0|H_{2B}|\phi_{-1}\rangle \\ \langle\phi_{-1}|H_{2B}|\phi_0\rangle & \langle\phi_{-1}|H_{2B}|\phi_{-1}\rangle \end{pmatrix} \tag{3}$$

The diagonalization of $H_{2\text{state}}$ yields the ground-state energy $E_{2B}(r^*)$ and the corresponding wave function $|\Psi_{2B}(r^*)\rangle$.

The applicability of the quasi-1D effective potential [Eq. (1)] to our harmonically confined system requires $l_\perp/l_0$ to be small. The energy $E_{2B}(r^*)$ is plotted in Fig. 1 (bottom) for $l_\perp/l_0 = 0.4$. Including more harmonic oscillator states in the basis allows for the calculation of higher-energy states (Fig. 2, bottom). However, it does not affect the qualitative behavior of the ground-state energy $E_{2B}(r^*)$ as long as $|\phi_{-1}\rangle$ is also included (Fig. 2, top).

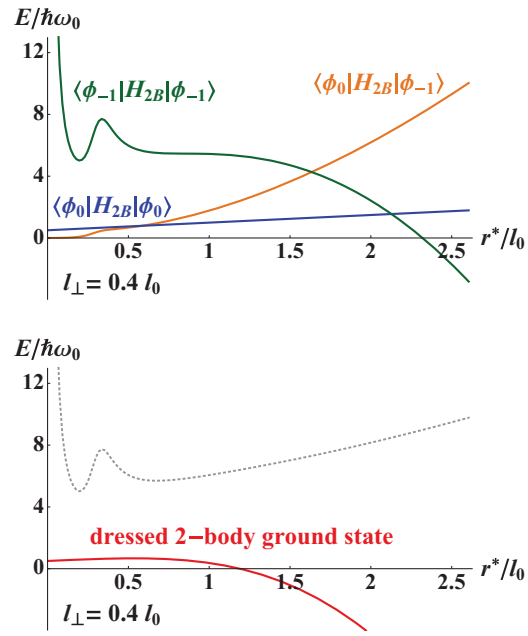

FIG. 1. (Color online) Top: Matrix elements of the two-state Hamiltonian $H_{2\text{state}}$ describing two bosonic dipoles in a harmonic trap, as a function of the dipolar length r^*. Bottom: Corresponding ground-state (red) and excited-state (dashed gray) energies.

The nonmonotonic behavior of $E_{2B}(r^*)$ is a signature of the DIR. The ground-state energy goes below $\hbar\omega_0/2$ for $r^* > r^*_{\text{crit}}$, where $r^*_{\text{crit}}/l_0 = 0.90$ for $l_\perp/l_0 = 0.4$. In the

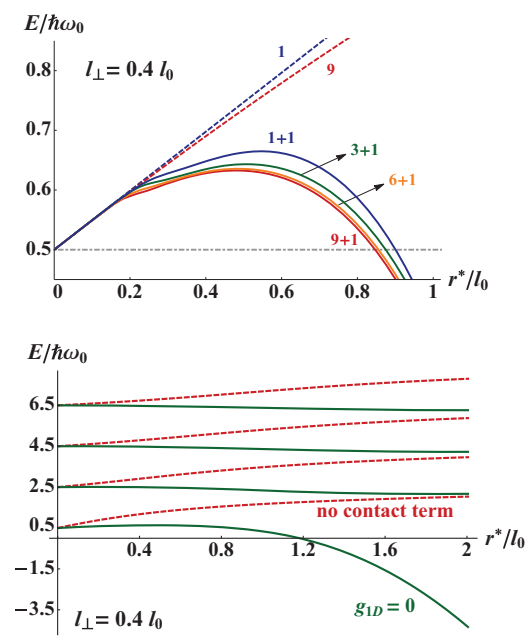

FIG. 2. (Color online) Top: Ground-state energy $E_{2B}(r^*)$ of the Hamiltonian H_{2B}, for $g_{1D} = 0$ and $l_\perp/l_0 = 0.4$, including 1 (blue), 3 (green), 6 (orange), and 9 (red) harmonic oscillator states, without (dashed lines) and with (solid lines) the bare bound state $|\phi_{-1}\rangle$ in the projection basis. Bottom: The four lowest eigenvalues of H_{2B} as a function of r^*, for $g_{1D} = 0$ (green) and choosing $g_{1D} = 2\hbar^2 r^*/(3ml_\perp^2)$ to cancel the contact term (dashed red), calculated including six harmonic oscillator states and the bare bound state $|\phi_{-1}\rangle$ in the basis.

many-body treatment described below, we are interested in situations where the dimer population is very small. Similarly to Feshbach resonance physics [35], the existence of the closed channel has a strong impact even though it is only marginally populated. Moreover, the dimer population being nearly vanishing will help us simplify the problem to an effective open-channel model. This assumption is satisfied here, as the overlap $|\langle\phi_{-1}|\Psi_{2B}\rangle|^2$ remains smaller than 0.10 for $r^* \lesssim r^*_{\rm crit}$. This overlap only becomes substantial if $|\phi_0\rangle$ and $|\phi_{-1}\rangle$ have comparable energies, i.e., for $r^*/l_0 \gtrsim 2.13$ (Fig. 1, top). The bound-state population near $r^*_{\rm crit}$ increases as $l_\perp/l_0$ decreases, but it remains <0.15 for $l_\perp/l_0 \geqslant 0.2$.

Figure 2 (bottom) shows the r^*-dependence of the lowest eigenvalues of $H_{2\rm B}$ in two different situations: (i) the s-wave interaction term $g_{1\rm D} = 0$ and (ii) $g_{1\rm D} \neq 0$ cancels the contact term in Eq. (1) completely [17]. The r^* dependence of the energy levels in these two situations is completely different. This will allow for an observation of the DIR using spectroscopic techniques [39].

III. MANY-BODY PHYSICS

We now consider N dipolar particles in a deep quasi-1D optical lattice with unity filling factor. We describe this system using a Bose-Hubbard model [10,40] extended to include nearest-neighbor interactions. We focus on the regime $r^* \lesssim r^*_{\rm crit}$, so that the DIR affects the two-body properties even though the number of dimers present in the system is extremely small. In order to properly account for the resonance, we start from the two-state description introduced above for the two-body problem [Eq. (3)]. Each of the two states $|\phi_0\rangle$ and $|\phi_{-1}\rangle$ yields a band and, hence, we introduce an atom-dimer EBHM whose Hamiltonian reads

$$\begin{aligned} H_{\rm AD} = \sum_i \Big[& \varepsilon_a n_i + \frac{U}{2} n_i(n_i-1) - J_a(a_i^\dagger a_{i+1} + \text{H.c.}) \\ & + V n_i n_{i+1} + \varepsilon_d m_i - J_d(b_i^\dagger b_{i+1} + \text{H.c.}) \\ & + \Omega(b_i^\dagger a_i a_i + \text{H.c.}) \Big]. \end{aligned} \tag{4}$$

In Eq. (4), $a_i^\dagger$ and $b_i^\dagger$ are the creation operators in the site i for atoms and dimers, respectively, and $n_i = a_i^\dagger a_i$ and $m_i = b_i^\dagger b_i$ are the corresponding number operators. Atoms and dimers are created in the ground state of the well i. The atomic tunneling coefficient J_a is taken from Ref. [41]. The atomic on-site and nearest-neighbor interaction parameters U and V are defined in terms of $V_{1\rm D}$ and the Wannier wave functions $w_i(x)$ and $w_{i+1}(x)$ localized on the sites i and $i+1$ by [30]

$$U = \iint dx_1 dx_2\, w_i^2(x_1) w_i^2(x_2)\, V_{1\rm D}(x_1 - x_2), \tag{5a}$$

$$V = \iint dx_1 dx_2\, w_i^2(x_1) w_{i+1}^2(x_2)\, V_{1\rm D}(x_1 - x_2). \tag{5b}$$

We use the Gaussian approximation to the Wannier functions $w_i(x)$. The on-site energy for atoms and dimers, ε_a and ε_d, the atomic on-site interaction energy U, and the atom-dimer conversion rate Ω can then all be expressed in terms of the matrix elements appearing in Eq. (3), namely,

$$\varepsilon_a = \frac{1}{2}\hbar\omega_0, \tag{6a}$$

$$\varepsilon_d = \varepsilon_a + \langle\phi_{-1}|H_{2\rm B}|\phi_{-1}\rangle, \tag{6b}$$

$$U = \langle\phi_0|H_{2\rm B}|\phi_0\rangle - \varepsilon_a, \tag{6c}$$

$$\Omega = \frac{1}{\sqrt{2}}\langle\phi_{-1}|H_{2\rm B}|\phi_0\rangle. \tag{6d}$$

The nearly vanishing dimer population allows for a crude description of the dimer dynamics; therefore we neglect atom-dimer and dimer-dimer interaction, and we take $J_d = J_a/10$.[2]

We focus on the tight-binding regime and we introduce the harmonic oscillator length l_0 characterizing the bottom of each lattice well. Like for the two-body problem, we consider a fixed and small value of $l_\perp/l_0$. The ground state of the system then depends on two adimensional parameters: r^*/l_0 and V/U. The choice of the parameter r^*/l_0 allows for a direct comparison with the two-body physics illustrated in Figs. 1 and 2. Assuming $g_{1\rm D} = 0$, Eqs. (5) show that the ratio V/U does not depend on r^*. It decays with the lattice depth $s = V_{\rm lat}/E_R$, where $V_{\rm lat}$ is the intensity of the optical lattice and E_R is the recoil energy. The harmonic approximation requires s to be large enough and thus imposes an upper bound on V/U.

For given values of r^*/l_0 and V/U, we numerically calculate the ground state of $H_{\rm AD}$ by exact diagonalization of a six-atom, six-well system. Figure 3 shows the phase diagram of the system for $l_\perp/l_0 = 0.4$. The observable is the single-particle off-diagonal density matrix element $\rho_1 = \langle a_2^\dagger a_1\rangle$, and it distinguishes the superfluid phase ($\rho_1 \neq 0$) from the insulating phases ($\rho_1 = 0$). The different insulating phases can subsequently be told apart by examining the ground-state wave function. Figure 3 compares the physically accessible phase diagram obtained using the single-band EBHM [23] [taking $\Omega = 0$ in Eq. (4)] with the atom-dimer phase diagram ($\Omega \neq 0$). In the considered range of parameters, the previously investigated single-band phase diagram exhibits two phases: SF and MI. The atom-dimer phase diagram presents three qualitative differences. First, the MI phase region stops at $r^* = r^*_{\rm crit}$. Second, the phase diagram includes a narrow MDW domain which occurs for very small values of V/U.[3] Third, there appears a "collapse" phase where all atoms sit in the same well.[4] In our small-sized system, the MI-MDW and

[2]This choice for J_d reflects the assumption that the polarizability of a molecule is twice that of an atom [41]. In the considered regime, its exact value does not affect our numerical results.

[3]Up to now, the MDW phase had been predicted to occur in an extended domain corresponding to large values of V/U [23].

[4]This collapse phase is related to the one predicted in the 2D case [42] using a mean-field approach to calculate the Bose-Hubbard parameters. Our phase diagram shows no phase with a period of three sites or more. We have checked that longer-period insulating phases are not energetically favored. This is in agreement with the density matrix renormalization group (DMRG) calculations including next-nearest-neighbor interactions reported in Ref. [24]. However, such phases have been predicted to occur for filling factors $\neq 1$ (see, e.g., Ref. [43]).

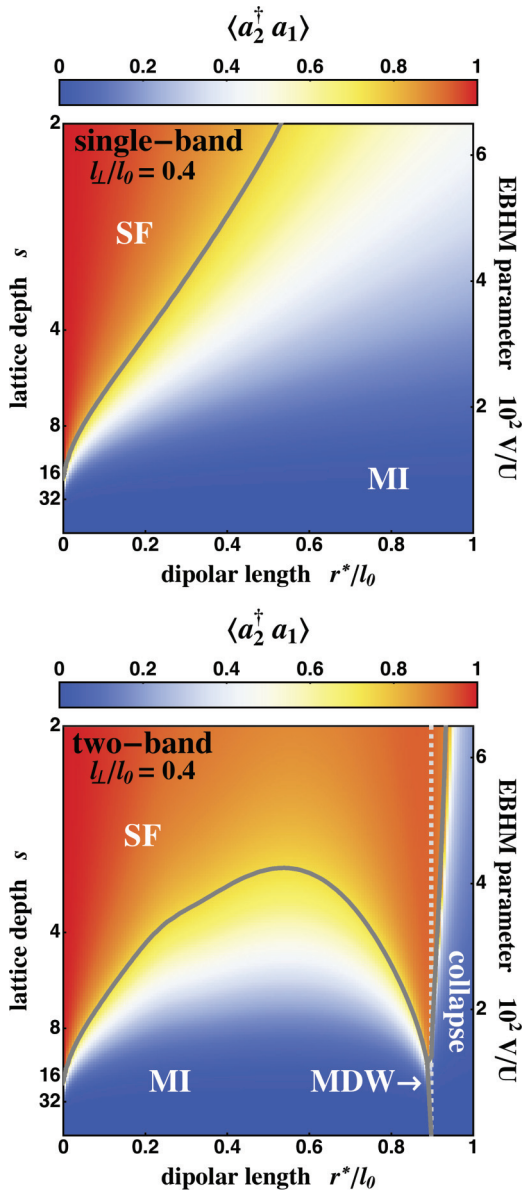

FIG. 3. (Color online) Many-body phase diagrams obtained using the single-band ($\Omega = 0$, top) and atom-dimer ($\Omega \neq 0$, bottom) EBHMs, performing exact diagonalization on a six-atom, six-well system with $l_\perp/l_0 = 0.4$. The effective on-site interaction $U_{\rm eff} < 0$ on the right of the vertical dashed line.

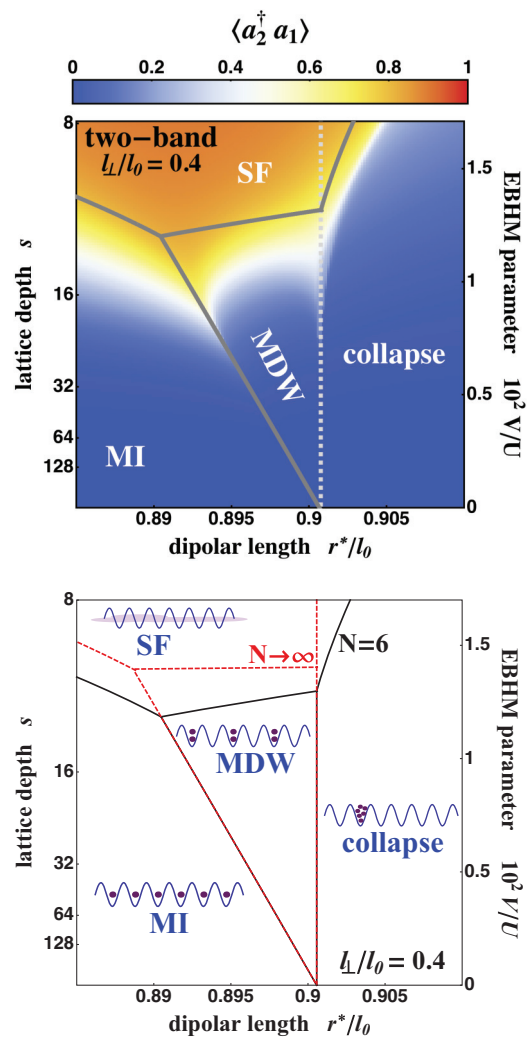

FIG. 4. (Color online) Top: Zoom-in on the part of the atom-dimer phase diagram [Fig. 3 (bottom), $l_\perp/l_0 = 0.4$] showing the transitions between the SF, MI, MDW, and collapse phases. Bottom: Quasianalytical phase boundaries calculated for $N = 6$ (solid black) and $N \to \infty$ (dashed red).

MDW-collapse transitions appear sharp, in accordance with their expected first-order character. Instead, the transitions between the SF phase and each insulating phase are smooth, which is compatible with the Berezinskii-Kosterlitz-Thouless behavior predicted in 1D [23].

Figure 5 shows a zoom-in on the atom-dimer phase diagrams for $l_\perp/l_0 = 0.3$ and 0.2. The comparison between Figs. 4 and 5 shows that decreasing the value of $l_\perp/l_0$ has a twofold effect on the phase diagram: (i) the collapse phase, which starts at $r^* = r^*_{\rm crit}$, appears for smaller values of r^*/l_0, and (ii) the extent of the MDW phase domain is reduced. This second result suggests that the experimental observation of MDW phases in quasi-1D bosonic systems will be difficult.

The phase diagram can be interpreted using an effective single-band EBHM, where the on-site interaction reproduces the two-body ground-state energy:

$$H_{\rm eff} = \sum_i \Big[-J_a(a_i^\dagger a_{i+1} + {\rm H.c.}) + \varepsilon_a n_i + \frac{1}{2} U_{\rm eff} n_i(n_i - 1) + V n_i n_{i+1} \Big], \tag{7}$$

with $U_{\rm eff}(r^*) = E_{\rm 2B}(r^*) - \varepsilon_a$. In the parameter range explored in Figs. 3 and 4, the phase diagram obtained using $H_{\rm eff}$ is very similar to the atom-dimer phase diagram. This is due to the atom-dimer detuning $\Delta = \varepsilon_d - U - 2\varepsilon_a$ being much larger than Ω, J_a, and V.[5] The effective model $H_{\rm eff}$ allows for a

[5]The two approaches are expected to yield different results for small Δ. Then, the dimer population is non-negligible, and the physics is described by the atom-dimer model of Eq. (4) where the parameters modeling the dimer dynamics should be properly chosen.

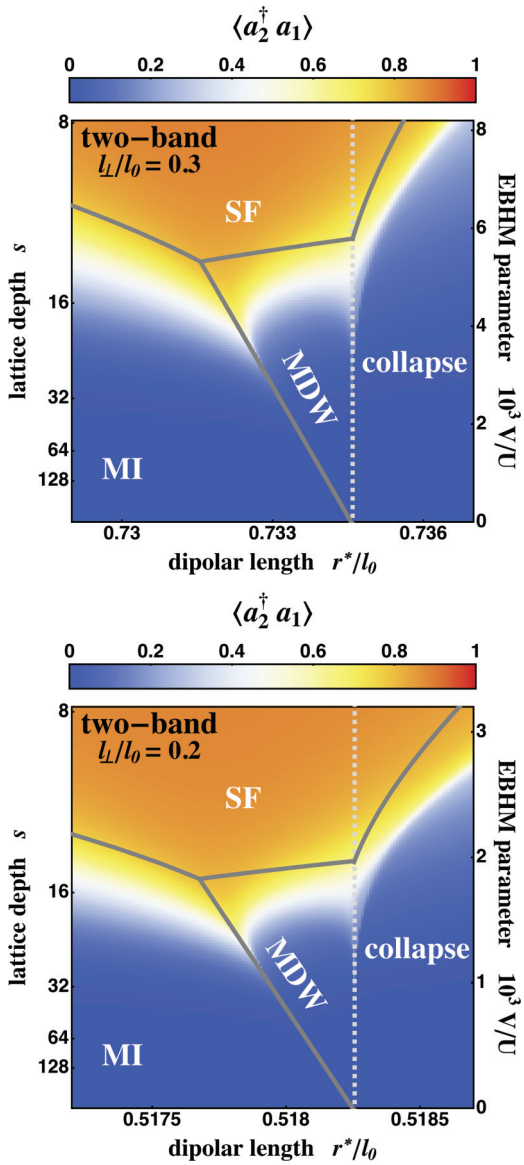

FIG. 5. (Color online) Zoom-in on the atom-dimer phase diagrams for $l_\perp/l_0 = 0.3$ (top) and $l_\perp/l_0 = 0.2$ (bottom).

comparison between our phase diagram and those calculated in terms of the EBHM parameters U/J and V/J. In particular, we find a Haldane-like phase near the upper left corner of our MDW domain, in agreement with the Haldane domain reported in Ref. [25].[6]

[6]A systematic investigation of the Haldane phase domain will be carried out on larger systems using DMRG.

We also use the effective single-band model to derive quasianalytical approximations for the phase boundaries for any number N of particles and sites. We calculate the energy deep within each phase in terms of J, $U_{\rm eff}$, V, and N. Equating these energies for two contiguous phases, we obtain the boundaries shown for $N = 6$ on Figs. 3 and 4 and for $N \to \infty$ on Fig. 4 (right). The boundaries found for $N = 6$ and for $N \to \infty$ are very similar. We now focus on the boundary between the SF and the collapse phases, given by $E_{\rm SF} - E_{\rm collapse} \approx N(V - 2J) - N^2 U_{\rm eff}/2 = 0$. The tunneling term scales with N, whereas the interaction scales with N^2. Hence, for small N, the superfluid phase survives in a region where $U_{\rm eff} < 0$, but the collapse phase is energetically favored for large N. This instability corresponds to the implosion of a BEC with a negative scattering length when its size is increased [44].

IV. OUTLOOK

The phase diagram which we have obtained describes the ground state of the system. One possible way to explore it experimentally is to cool the system in a given geometry in the absence of dipolar interactions and then adiabatically increase r^*. The phases we have predicted at $T = 0$ may be experimentally identified using *in situ* imaging techniques as well as the recent advances allowing for the detection of nonlocal order [45]. The narrow MDW domain which appears in the phase diagram for small V/U is well within the validity range of our atom-dimer Hamiltonian. By contrast, the MDW phase domain previously predicted using the standard EBHM [23,25] occurs in an extended domain corresponding to large values of V/U.

The DIR could also have a strong effect on systems described by generalized EBHMs such as the one studied in Ref. [14]. It would be interesting to extend this work to 2D geometries, where the anisotropy of the dipolar interaction is expected to play a role. Our analysis would also be relevant for the understanding of the fermionic 1D EBHM with repulsive interactions, where the relevant phases are the spin density wave, the charge density wave, and the bond order wave [46–49].

ACKNOWLEDGMENTS

We acknowledge stimulating discussions with M. Baranov, G. Ferrari, L. P. Pitaevskii, G. V. Shlyapnikov, S. Stringari, and W. Zwerger. L.B. acknowledges the hospitality of the BEC Center, Trento, during the initial stage of the project. This work has been supported by ERC through a QGBE grant and by Provincia Autonoma di Trento.

[1] T. Lahaye, C. Menotti, L. Santos, M. Lewenstein, and T. Pfau, Rep. Prog. Phys. **72**, 126401 (2009).
[2] M. A. Baranov, M. Dalmonte, G. Pupillo, and P. Zoller, Chem. Rev. **112**, 5012 (2012).
[3] A. Griesmaier, J. Werner, S. Hensler, J. Stuhler, and T. Pfau, Phys. Rev. Lett. **94**, 160401 (2005).
[4] K. Aikawa, A. Frisch, M. Mark, S. Baier, A. Rietzler, R. Grimm, and F. Ferlaino, Phys. Rev. Lett. **108**, 210401 (2012).

[5] M. Lu, N. Q. Burdick, S. H. Youn, and B. L. Lev, Phys. Rev. Lett. **107**, 190401 (2011).

[6] J. Stuhler, A. Griesmaier, T. Koch, M. Fattori, T. Pfau, S. Giovanazzi, P. Pedri, and L. Santos, Phys. Rev. Lett. **95**, 150406 (2005).

[7] K.-K. Ni, S. Ospelkaus, M. G. H. de Miranda, A. Pe'er, B. Neyenhuis, J. J. Zirbel, S. Kotochigova, P. S. Julienne, D. S. Jin, and J. Ye, Science **322**, 231 (2008).

[8] C.-H. Wu, J. W. Park, P. Ahmadi, S. Will, and M. W. Zwierlein, Phys. Rev. Lett. **109**, 085301 (2012).

[9] M. Saffman, T. G. Walker, and K. Molmer, Rev. Mod. Phys. **82**, 2313 (2010).

[10] I. Bloch, J. Dalibard, and S. Nascimbène, Nat. Phys. **8**, 267 (2012).

[11] M. H. G. de Miranda, A. Chotia, B. Neyenhuis, D. Wang, G. Quéméner, S. Ospelkaus, J. L. Bohn, J. Ye, and D. S. Jin, Nat. Phys. **7**, 502 (2011).

[12] U. R. Fischer, Phys. Rev. A **73**, 031602 (2006).

[13] N. Matveeva and S. Giorgini, Phys. Rev. Lett. **109**, 200401 (2012); Z.-K. Lu and G. V. Shlyapnikov, Phys. Rev. A **85**, 023614 (2012); M. Babadi and E. Demler, Phys. Rev. B **84**, 235124 (2011); M. Babadi, B. Skinner, M. M. Fogler, and E. Demler, arXiv:1212.1493.

[14] T. Sowinski, O. Dutta, P. Hauke, L. Tagliacozzo, and M. Lewenstein, Phys. Rev. Lett. **108**, 115301 (2012).

[15] A. Pikovski, M. Klawunn, G. V. Shlyapnikov, and L. Santos, Phys. Rev. Lett. **105**, 215302 (2010); N. Zinner, B. Wunsch, D. Pekker, and D.-W. Wang, Phys. Rev. A **85**, 013603 (2012); M. Klawunn and A. Recati, *ibid.* **88**, 013633 (2013); C.-K. Chan, C. Wu, W.-C. Lee, and S. Das Sarma, *ibid.* **81**, 023602 (2010).

[16] S. Sinha and L. Santos, Phys. Rev. Lett. **99**, 140406 (2007).

[17] F. Deuretzbacher, J. C. Cremon, and S. M. Reimann, Phys. Rev. A **81**, 063616 (2010); **87**, 039903(E) (2013).

[18] A. Maluckov, G. Gligoric, L. Hadzievski, B. A. Malomed, and T. Pfau, Phys. Rev. Lett. **108**, 140402 (2012).

[19] A. G. Volosniev, J. R. Armstrong, D. V. Fedorov, A. S. Jensen, M. Valiente, and N. T. Zinner, New J. Phys. **15**, 043046 (2013).

[20] B. Pasquiou, G. Bismut, E. Maréchal, P. Pedri, L. Vernac, O. Gorceix, and B. Laburthe-Tolra, Phys. Rev. Lett. **106**, 015301 (2011).

[21] A. Chotia, B. Neyenhuis, S. A. Moses, B. Yan, J. P. Covey, M. Foss-Feig, A. M. Rey, D. S. Jin, and J. Ye, Phys. Rev. Lett. **108**, 080405 (2012).

[22] B. Yan, S. A. Moses, B. Gadway, J. P. Covey, K. R. A. Hazzard, A. M. Rey, D. S. Jin, and J. Ye, arXiv:1305.5598.

[23] R. V. Pai and R. Pandit, Phys. Rev. B **71**, 104508 (2005).

[24] E. G. Dalla Torre, E. Berg, and E. Altman, Phys. Rev. Lett. **97**, 260401 (2006).

[25] D. Rossini and R. Fazio, New J. Phys. **14**, 065012 (2012).

[26] H. P. Büchler, Phys. Rev. Lett. **104**, 090402 (2010).

[27] M. Marinescu and L. You, Phys. Rev. Lett. **81**, 4596 (1998).

[28] Z. Y. Shi, R. Qi, and H. Zhai, Phys. Rev. A **85**, 020702 (2012).

[29] R. Qi, Z.-Y. Shi, and H. Zhai, Phys. Rev. Lett. **110**, 045302 (2013).

[30] C. Trefzger, C. Menotti, B. Capogrosso-Sansone, and M. Lewenstein, J. Phys. B **44**, 193001 (2011).

[31] I. Bloch, J. Dalibard, and W. Zwerger, Rev. Mod. Phys. **80**, 885 (2008).

[32] K. Kanjilal and D. Blume, Phys. Rev. A **78**, 040703 (2008).

[33] T. M. Hanna, E. Tiesinga, W. F. Mitchell, and P. S. Julienne, Phys. Rev. A **85**, 022703 (2012).

[34] D. S. Petrov, G. V. Shlyapnikov, and J. T. M. Walraven, Phys. Rev. Lett. **85**, 3745 (2000).

[35] C. Chin, R. Grimm, P. Julienne, and E. Tiesinga, Rev. Mod. Phys. **82**, 1225 (2010).

[36] T. Koch, T. Lahaye, J. Metz, B. Fröhlich, A. Griesmaier, and T. Pfau, Nat. Phys. **4**, 218 (2008).

[37] M. Olshanii, Phys. Rev. Lett. **81**, 938 (1998).

[38] T. Busch, B. Englert, K. Rzazewski, and M. Wilkens, Found. Phys. **28**, 549 (1998).

[39] J. Hecker-Denschlag, J. E. Simsarian, H. Häffner, C. McKenzie, A. Browaeys, D. Cho, K. Helmerson, S. L. Rolston, and W. D. Phillips, J. Phys. B **35**, 3095 (2002).

[40] M. P. A. Fisher, P. B. Weichman, G. Grinstein, and D. S. Fisher, Phys. Rev. B **40**, 546 (1989).

[41] F. Gerbier, A. Widera, S. Fölling, O. Mandel, T. Gericke, and I. Bloch, Phys. Rev. A **72**, 053606 (2005), typo corrected.

[42] K. Goral, L. Santos, and M. Lewenstein, Phys. Rev. Lett. **88**, 170406 (2002).

[43] F. Burnell, M. M. Parish, N. R. Cooper, and S. L. Sondhi, Phys. Rev. B **80**, 174519 (2009).

[44] E. A. Donley, N. R. Claussen, S. L. Cornish, J. L. Roberts, E. A. Cornell, and C. E. Wieman, Nature **412**, 295 (2001).

[45] M. Endres, M. Cheneau, T. Fukuhara, C. Weitenberg, P. Schauss, C. Gross, L. Mazza, M. C. Banuls, L. Pollet, I. Bloch, and S. Kuhr, Science **334**, 200 (2011).

[46] S. Ejima and S. Nishimoto, Phys. Rev. Lett. **99**, 216403 (2007).

[47] M. Nakamura, Phys. Rev. B **61**, 16377 (2000).

[48] S. G. Bhongale, L. Mathey, S.-W. Tsai, C. W. Clark, and E. Zhao, Phys. Rev. Lett. **108**, 145301 (2012).

[49] M. D. Dio, L. Barbiero, M. Dalmonte, and A. Recati, arXiv:1304.5200.